Notes: 2D dynamical systems

Sebastian Boie

For any questions or suggestions about the notes, please e-mail me at
sdb2008@med.cornell.edu

Characterization of the stability of equilibria

We derive a diagram that is useful for the characterization of the stability of equilibria in 2D systems. Assume that we have a system of the form

$$\begin{aligned} \frac{dx}{dt} &= f(x,y), \\ \frac{dy}{dt} &= g(x,y), \end{aligned} \tag{1}$$

which has an equilibrium at $(x_{\text{eq}}, y_{\text{eq}}) = (0,0)$. We get the stability of the equilibrium by linearizing equation (1) around $(x_{\text{eq}}, y_{\text{eq}})$. The Jacobian is

$$J = \begin{pmatrix} D_x f & D_y f \\ D_x g & D_y g \end{pmatrix}. \tag{2}$$

The eigenvalues of the Jacobian evaluated at $(x_{\text{eq}}, y_{\text{eq}})$ determines the stability of the equilibrium. In order to get the eigenvalues we calculate:

$$\begin{aligned} 0 &= \det \begin{pmatrix} D_x f - \lambda & D_y f \\ D_x g & D_y g - \lambda \end{pmatrix} \\ &= (D_x f - \lambda)(D_y g - \lambda) - D_y f D_x g \\ &= \lambda^2 - (D_x f + D_y g)\lambda + D_x f D_y g - D_x g D_y f \\ &= \lambda^2 - \operatorname{tr}(J)\lambda + \det(J) \end{aligned}$$

Hence the eigenvalues are

$$\lambda_{1,2} = \frac{\operatorname{tr}(J(x_{\text{eq}}, y_{\text{eq}}))}{2} \pm \sqrt{\operatorname{tr}^2(J(x_{\text{eq}}, y_{\text{eq}})) - 4\det(J(x_{\text{eq}}, y_{\text{eq}}))}. \tag{3}$$

Based on the relationship between trace and determinant we find 5 different regimes as shown in Fig.(1). Above the parabola (given by $\operatorname{tr}^2(J) = 4\det(J)$) the eigenvalues are complex conjugate. This indicates that trajectories will have a rotational component in the vicinity of the equilibrium. In the upper right quadrant ($\det(J) > 0, \operatorname{tr}(J) > 0$) equilibria are stable, in the upper left quadrant ($\det(J) > 0, \operatorname{tr}(J) < 0$) equilibria are unstable. In the lower halfplane ($\det(J) < 0$) equilibria are neither stable nor unstable, but have a stable direction and an unstable direction.

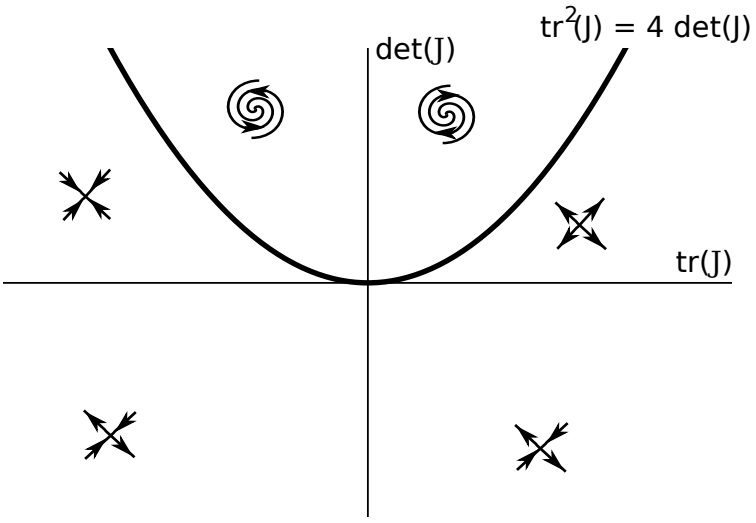

Figure 1: Different stability regimes based on $\det(J)$ and $\mathrm{tr}(J)$.

First example: Olfactory path following model

In this section we study a simple toy model of a navigator that is tracking an odor trail in two dimensions (*e.g.* a walking fly following an odor trail on a table). The model assumptions are, that the navigator:

- travels at constant velocity v,
- has sensors at the end of two antennae of length l separated by angle $0 < \theta < \pi$,
- compares the concentration difference between the two sensors and turns towards the higher concentration.

A sketch of the navigator is shown in Fig.(2). The first two equations of motion in Eq.(4) can be derived by projecting the current heading direction on the axes and multiplying with the constant velocity v. The third equation is just the difference of the odor concentration across antennae multiplied by a gain factor α.

$$\begin{aligned} \frac{dx}{dt} &= v\cos\phi \\ \frac{dy}{dt} &= v\sin\phi \\ \frac{d\phi}{dt} &= \alpha(C(x_L, y_L) - C(x_R, y_R)) \end{aligned} \tag{4}$$

The coordinates of the antennae with respect to the fixed coordinate axes can be derived by

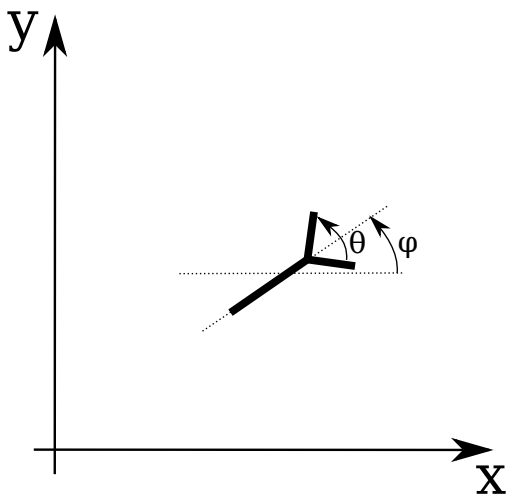

Figure 2: Sketch of toy navigator.

trigonometry (no magic involved):

$$\begin{aligned} x_L &= x + l\cos\left(\phi + \frac{\theta}{2}\right), \\ y_L &= y + l\sin\left(\phi + \frac{\theta}{2}\right), \\ x_R &= x + l\cos\left(\phi - \frac{\theta}{2}\right), \\ y_R &= y + l\sin\left(\phi - \frac{\theta}{2}\right). \end{aligned} \tag{5}$$

We need to specify the odor trail. Let's assume that the odor concentration is constant in time and spread out like a gaussian. We can align our coordinate system such that the trail is laid out along one of the coordinate axes. For example, consider a gaussian profile in x-direction, which is constant in the y-direction. Then, the odor concentration is given by:

$$C(x, y) = C_{\max} \exp\left[-\frac{x^2}{2\sigma^2}\right], \tag{6}$$

and can be seen as a heatplot in Fig.(3). Substituting the equation for the odor trail (Eq.(6)) and the location of the antennae Eq.(5) into the system 4 we get the full system:

$$\begin{aligned} \frac{dx}{dt} &= v\cos\phi, \\ \frac{dy}{dt} &= v\sin\phi, \\ \frac{d\phi}{dt} &= \alpha C_{\max}\left(\exp\left[-\frac{\left(x^2 + l\cos\left(\phi + \frac{\theta}{2}\right)\right)^2}{2\sigma^2}\right] - \exp\left[-\frac{\left(x^2 + l\cos\left(\phi - \frac{\theta}{2}\right)\right)^2}{2\sigma^2}\right]\right). \end{aligned} \tag{7}$$

After specifying the initial condition (x_0, y_0, ϕ_0) we could solve (integrate) the model and study its behavior. However, an important thing to note is that the right-hand side of Eq.(7) is independent

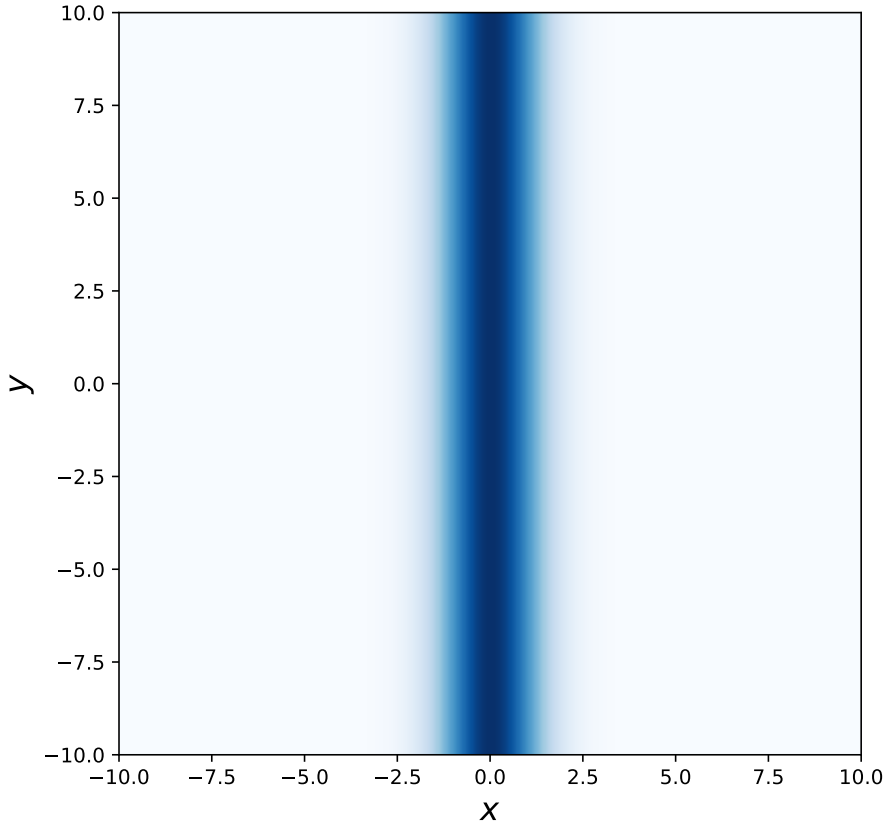

Figure 3: Concentration profile of the odor trail for $C_{\max} = 10, \sigma = 1$.

of y. Hence the dynamics of the navigator are independent of the value of y and the dynamics are determined by the evolution of x and ϕ alone. In order to understand the behavior of the model, we could ask the question:

Does the system have equilibria?

The full system cannot have equilibria, since $v\sin(\phi)$ and $v\cos(\phi)$ cannot be simultaneously zero for $v > 0$. However, we can ask the question whether the two-dimensional system of $\frac{dx}{dt}, \frac{d\phi}{dt}$ has equilibria.

The first equation needs to satisfy $v\cos\phi = 0$, hence $\phi = \pi/2$ or $\phi = 3\pi/2$. Substituting into the equation for $d\phi/dt$:

$$\begin{aligned}\frac{d\phi}{dt} &= \alpha C_{max}\left\{\exp\left[-\frac{\left(x + l\cos\left(\frac{\theta}{2}+\frac{\pi}{2}\right)\right)^2}{2\sigma^2}\right] - \exp\left[-\frac{\left(x + l\cos\left(\frac{\theta}{2}-\frac{\pi}{2}\right)\right)^2}{2\sigma^2}\right]\right\} \\ &= \alpha C_{max}\left\{\exp\left[-\frac{\left(x - l\sin\frac{\theta}{2}\right)^2}{2\sigma^2}\right] - \exp\left[-\frac{\left(x + l\sin\frac{\theta}{2}\right)^2}{2\sigma^2}\right]\right\},\end{aligned} \tag{8}$$

where in the second step we just used the fact that $\pm\frac{\pi}{2}$ shifts the cosine left or right, which turns it into $\mp\sin\left(\frac{\theta}{2}\right)$. Likewise, for $\phi = 3\pi/2$, the minus sign in the numerator of the exponents switches. Eq.(8) can only be zero when the exponents are equal. Expanding the numerator of the exponents

yields

$$\left(x - l\sin\frac{\theta}{2}\right)^2 = x^2 - 2xl\sin\frac{\theta}{2} + l^2\sin^2\frac{\theta}{2},$$
$$\left(x + l\sin\frac{\theta}{2}\right)^2 = x^2 + 2xl\sin\frac{\theta}{2} + l^2\sin^2\frac{\theta}{2}.$$

For fixed $0 < \theta < \pi$ the two exponents can only be equal for $x = 0$.

The next thing we would like to know is what the stability of the equilibria is. The Jacobian is of the form

$$J(x,\phi) = \begin{pmatrix} 0 & -v\sin\phi \\ \dfrac{\partial}{\partial x}\left(\dfrac{d\phi}{dt}\right) & \dfrac{\partial}{\partial \phi}\left(\dfrac{d\phi}{dt}\right) \end{pmatrix},$$

hence $\mathrm{tr}(J) = \frac{\partial}{\partial\phi}\left(\frac{d\phi}{dt}\right)$ and $\det(J) = v\sin\phi\frac{\partial}{\partial x}\left(\frac{d\phi}{dt}\right)$. The algebra is cumbersome but straightforward. It turns out that:

$$\begin{aligned}
\mathrm{tr}\ J\left(0,\frac{\pi}{2}\right) &< 0,\\
\mathrm{tr}^2\ J\left(0,\frac{\pi}{2}\right) &< 4\det J\left(0,\frac{\pi}{2}\right),\\
\mathrm{tr}\ J\left(0,\frac{3\pi}{2}\right) &< 0,\\
\mathrm{tr}^2\ J\left(0,\frac{3\pi}{2}\right) &< 4\det J\left(0,\frac{3\pi}{2}\right).
\end{aligned}$$

Hence both equilibria have complex conjugate eigenvalues with negative real part. Thus, in the vicinity of the equilibria trajectories are spiraling in (see Fig.6). The spiraling motion near the equilibria in the two-dimensional system correspond to trajectories that close in on the odor trail in an oscillating fashion (Fig.5) and follow the odor trail in positive or negative y-direction.

For the figures the parameters are:

$$\begin{aligned}
C_{\max} &= 10\\
\sigma &= 1\\
\alpha &= 1\\
l &= 0.1\\
\theta &= \frac{\pi}{4}\\
v &= 1
\end{aligned}$$

and the initial conditions $(x_0, y_0) = (2, 1)$ and $\phi_0 = 0.9 \cdot \frac{\pi}{2}$ and $\phi_0 = 3.1 \cdot \frac{\pi}{2}$.

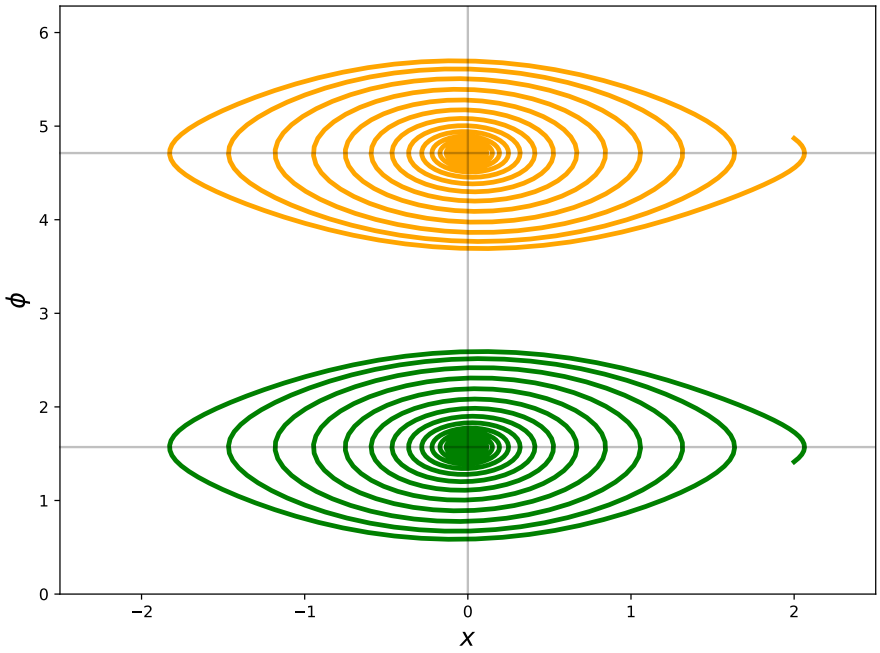

Figure 4: Equilibria are located at the crosses of the two grey shaded nullclines. Both are stable and trajectories within the basin of attraction spiral towards the equilibria.

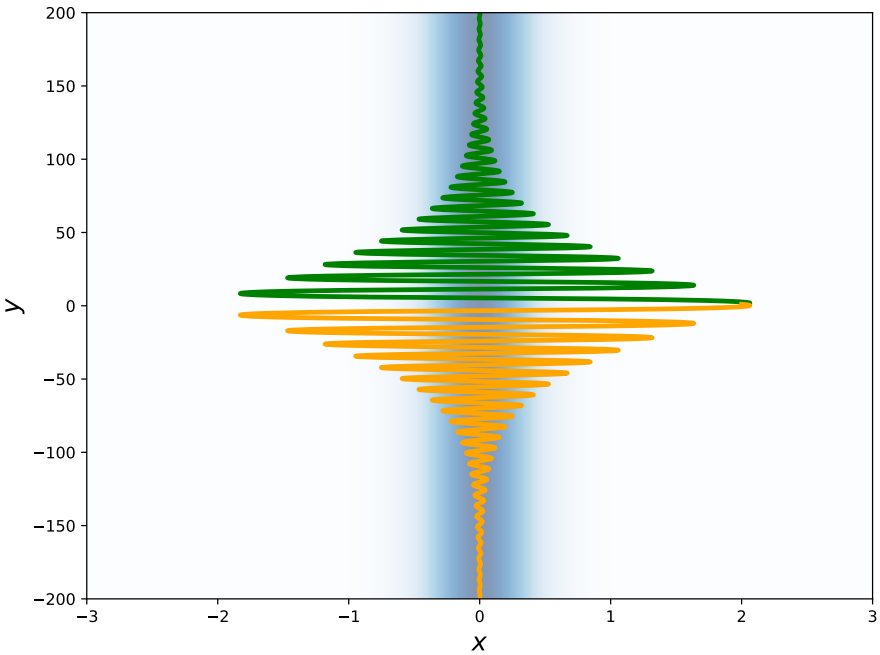

Figure 5: The equilibria of the 2D system of x and ϕ correspond to solution

Second example: FitzHugh-Nagumo model

The FitzHugh-Nagumo equations have been derived as a simple toy model for a spiking neuron[1]. The FitzHugh-Nagumo equations aim to capture the essential mathematical features that the Hodgkin-Huxley model for the squid giant axon shows. The equations are

$$\begin{aligned} \frac{dv}{dt} &= I_{\text{app}} + v - \frac{v^3}{3} - w, \\ \frac{dw}{dt} &= \epsilon\left(v - \alpha w + \beta\right), \end{aligned} \tag{9}$$

where v represents the membrane voltage and w a recovery variable. I_{app} is the applied current, α and β are non-negative parameters and $0 < \epsilon \ll 1$ acts as a timescale separation between the two equations. In order to get to grips with a nonlinear dynamical system it is common to check for equilibria, and in 2D, plot the nullclines. For the analysis we'll use $\epsilon = 0.01$, $\alpha = 0.5, \beta = 2$ and we'll consider variable applied currents I_{app}.

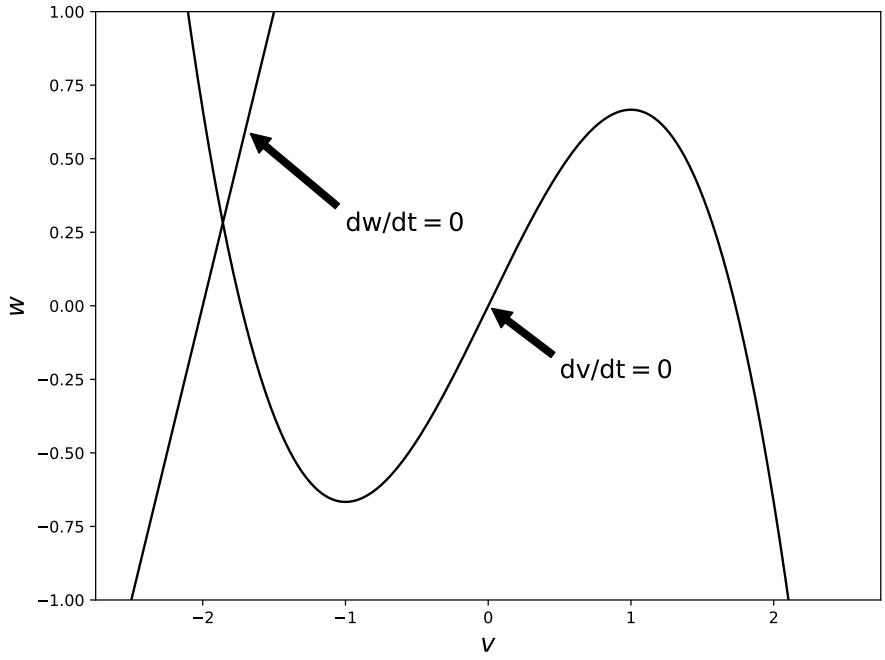

Figure 6: Nullclines. The intersection of the nullclines is an equilibrium.

For the given parameter values the two nullclines intersect at

$$\begin{aligned} v_{\text{eq}} &= -1.859, \\ w_{\text{eq}} &= 0.282, \end{aligned} \tag{10}$$

which is the only equilibrium of the system. At the equilibrium $\text{tr}\, J(v_{\text{eq}}, w_{\text{eq}}) < 0$ and $\text{tr}^2\, J(v_{\text{eq}}, w_{\text{eq}}) > 4 \det J(v_{\text{eq}}, w_{\text{eq}})$. Hence, we have a stable equilibrium which acts as a sink without spiralling motion of nearby trajectories.

There is a set of powerful numerical algorithms which allow to track equilibria and their stability as one or more parameters (in this case I_{app}) are varied.

[1] http://www.scholarpedia.org/article/FitzHugh-Nagumo

Digression: Implicit Function Theorem and Numerical Continuation

Suppose that f is a continuously differentiable function where

$$f : \mathbb{R}^{n+m} \to \mathbb{R}^m \quad \text{with} \quad f(x, y) = 0.$$

If $D_y f$ is invertible at point (a, b) where $f(a, b) = 0$, then there is an open neighborhood around (a, b) where $y = g(x)$ and $f(x, g(x)) = 0$.

The implicit function theorem guarantees that y can be written as a function of x in the vicinity of (a, b), although it does not provide a recipe for obtaining $g(x)$. However, it does provide the derivative via the calculation

$$0 = D_x f(x, g(x)) = D_x f + (D_y f) \frac{\partial g}{\partial x},$$
$$\frac{\partial g}{\partial x} = -(D_y f)^{-1} D_x f.$$

Provided that the implicit function theorem is satisfied, an equilibrium can be tracked as one varies a system parameter. We check for the FitzHugh-Nagumo equations if we can track the equilibrium $(v_{\text{eq}}, w_{\text{eq}})$ as we vary I_{app}. In order to this we look at the extended Jacobian

$$J_{I_{\text{app}},(v,w)} = \begin{pmatrix} 1 & 1 - v^2 & -1 \\ 0 & \epsilon & -\epsilon\alpha \end{pmatrix}$$

Hence if the submatrix $J_{(v,w)}$ is invertible, we can write the curve of equilibria, to first order, as

$$\begin{pmatrix} v_{\text{eq}} \\ w_{\text{eq}} \end{pmatrix} = G(0) + \frac{\partial G(0)}{\partial I_{\text{app}}} \cdot \Delta I_{\text{app}}.$$

This linear approximation is the basic idea for a set of powerful software packages that can follow equilibria and other invariant structures (*e.g.* periodic orbits) as one varies a parameter. The most well-known packages are

- AUTO, most widely used, fastest (written in Fortran and python),
- XPPAUT graphical user interface to AUTO (written in C, but no coding necessary),
- matcont (Matlab, most exhaustive bifurcation detection ability),
- coco (Matlab, very recent, promising).

None of these software packages is straightforward. If you would like to try to explore models with continuation tools, my first recommendation would be XPPAUT. There is an online tutorial available[2].

The results of following the equilibrium points as we vary I_{app} is shown in Fig.7. The left panel shows the location and stability of v_{eq}. Note that the equilibrium exhibits two changes of stability HB_1 and HB_2. At these Hopf bifurcations a parametric family of periodic orbits starts or terminates. The numerical continuation software can switch to the branches of periodic orbits. Switching to the branch of periodic, we can plot the amplitude (blue curve in the left panel) and the period of the resulting periodic orbits (right panel).

Note that the analysis of equilibria is only locally valid. In other words, it does not tell you about the behavior away from equilibrium solutions. For systems beyond two dimensions a global

[2] http://www.math.pitt.edu/~bard/xpp/xpp.html

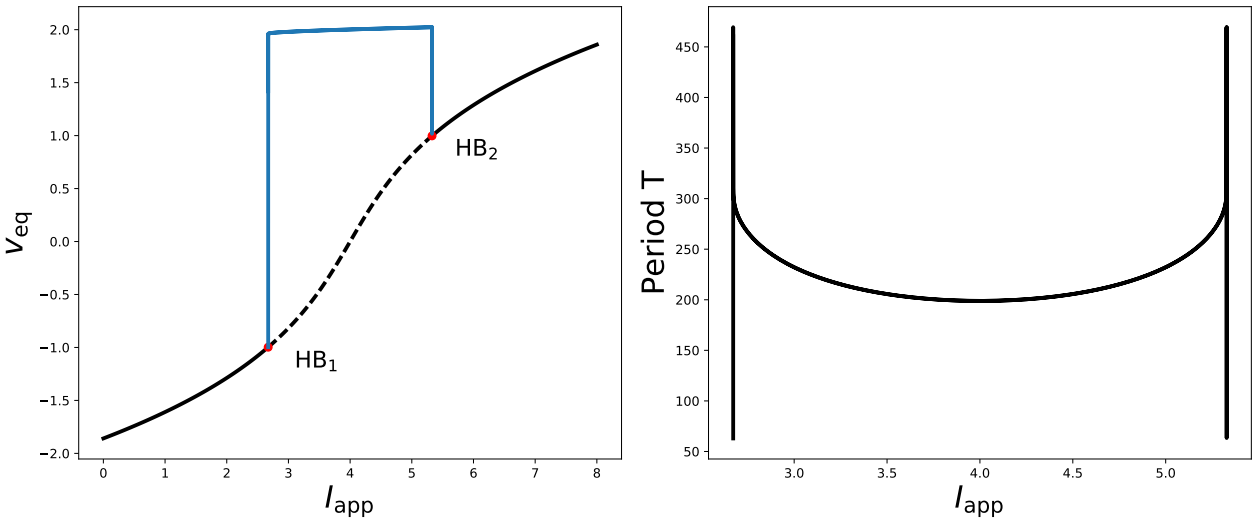

Figure 7: Following the equilibrium as we increase I_{app} shows two changes of stability at HB_1 and HB_2, from which periodic orbits emanate. The blue curve shows the amplitude of the periodic for a given value of I_{app}. Numerical continuation software has the ability to switch the branch to following the periodic orbit were they exist. The curve on the right shows how the period of the periodic orbit changes as I_{app} is varied.

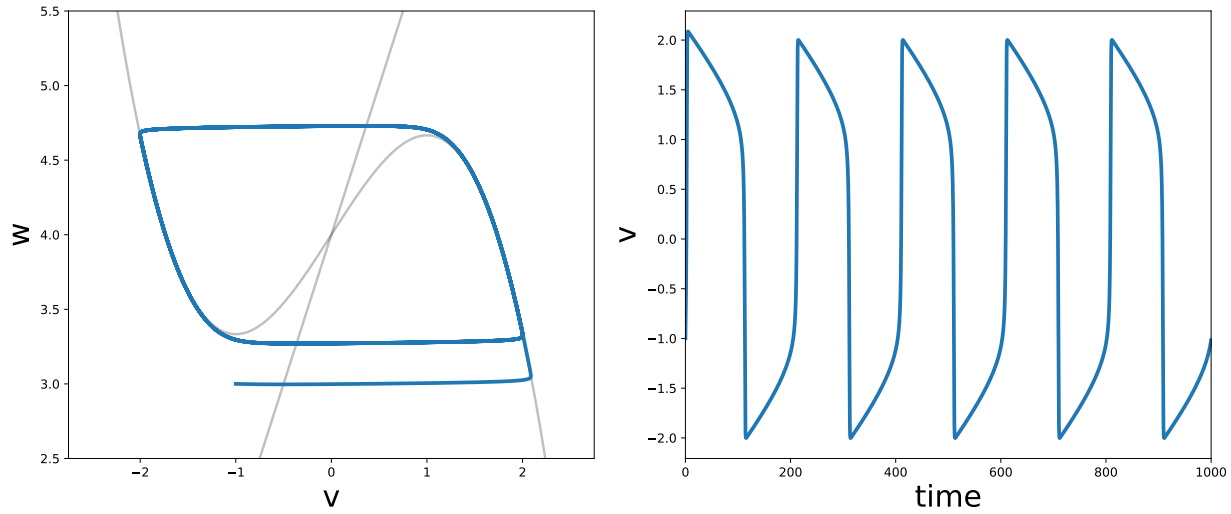

Figure 8: Simulation of the periodic at $I_{\text{app}} = 4$. Left figure shows the periodic orbit in phase space (in (v, w)-coordinates and the right figure shows the timeseries of the voltage variable.

analysis and a global understanding of the behavior of a model for different values of parameters is very challenging. However, the FitzHugh-Nagumo equations are one of the few nonlinear dynamical systems that can be globally understood. In order to do this, we look at a technique that allows us to consider slow and fast components of the dynamics separately.

Geometric singular perturbation theory

A thing to note is that we have the flexibility to rescale our time variable without changing the dynamics. A useful rescaling is $T = \epsilon t$ (I double checked). Then the derivatives become

$$\begin{aligned}\frac{dv}{dt} &= \frac{dv}{dT}\frac{dT}{dt} = \epsilon\frac{dv}{dT},\\ \frac{dw}{dt} &= \epsilon\frac{dw}{dT}.\end{aligned}$$

And the FitzHugh-Nagumo equations can be equivalently written as

$$\begin{aligned}\epsilon\frac{dv}{dT} &= I_{\text{app}} + v - \frac{v^3}{3} - w,\\ \frac{dw}{dT} &= (v - \alpha w + \beta).\end{aligned} \tag{11}$$

Equations (11) and (9) are equivalent, showing the system's dynamics with differently scaled time variables. However, if we treat Eq.(11) and Eq.(9) as singular perturbation problems ($\lim \epsilon \to 0$) we get different limits. The limit of Eq. (9) is

$$\begin{aligned}\frac{dv}{dt} &= I_{\text{app}} + v - \frac{v^3}{3} - w,\\ \frac{dw}{dt} &= 0,\end{aligned}$$

which has an intuitive interpretation. If trajectories are away from $\frac{dv}{dt} \approx 0$ (where this limit is justified) the variables w can be considered as constants, and the evolution of the system is governed by the equation for v. The limit of Eq.(11) yields the differential-algebraic system

$$\begin{aligned}0 &= I_{\text{app}} + v - \frac{v^3}{3} - w,\\ \frac{dw}{dT} &= (v - \alpha w + \beta),\end{aligned}$$

which is a differential equation (dw/dT) subject to an algebraic constraint. This system is only meaningful on the so called *critical manifold*:

$$S_0 = \left\{(v, w) \in \mathbb{R}^2 \,\middle|\, I_{\text{app}} + v - \frac{v^3}{3} - w = 0\right\}$$

In the vicinity of the critical manifold, the equation dw/dT governs the dynamics.

Fenichel's theorem as stated below justifies mathematically that we can split this "slow-fast" system into slow and fast components, and that the corresponding limits, explain the dynamics for the model for $\epsilon > 0$.

Fenichel theorem

Suppose that $M_0 \subset S_0$ is compact and normally hyperbolic, that means that all eigenvalues λ of the Jacobian $\frac{\partial f}{\partial v}\Big|_{M_0}$ satisfy $\text{Re}(\lambda) \neq 0$. Furthermore, suppose that the right-hand functions are smooth, then there exists a manifold M_ϵ within distance $O(\epsilon)$ of M_0, which is locally invariant under the flow.

This theorem makes the idea rigorous that there is a lower dimensional slow manifold in the system and in the vicinity of this manifold, the system evolves on a slower timescale. This theorem is not restricted to two dimensions. For example the Hodgkin-Huxley equations have two fast and two slow variables and correspondingly, the manifold where evolution is slow, is two-dimensional.

For the FitzHugh-Nagumo equations the critical manifold is normally hyperbolic everywhere but at $v = \pm 1$, since $D_v \left(I_{\text{app}} + v - \frac{v^3}{3} - w \right) = 1 - v^2$, which correspond to the knees of the nullcline. Furthermore, the eigenvalue of the critical manifold is smaller than zero for $|v| > 1$ and larger than zero for $-1 < v < 1$. Correspondingly the critical manifold has two attracting and a repelling branch see Fig. 9. Using the singular perturbation approach, we can now explain the dynamics of this model globally. Away from the critical manifold, trajectories are moving rapidly towards one of the attracting branches of the critical manifold. Once the trajectory is on the critical manifold, the slow dynamics take over and evolve the system along the critical manifold until it reaches a stable equilibrium (for example when $I_{\text{app}} = 0$) or reaches a knee and jumps to the other attracting branch of the critical manifold. If the only equilibrium is an unstable equilibrium on the repelling branch (see Fig.8), then the globally attracting state is a periodic orbit where the trajectory jumps between the stable branches of the critical manifold and evolves slowly until it reaches the vicinity of a knee.

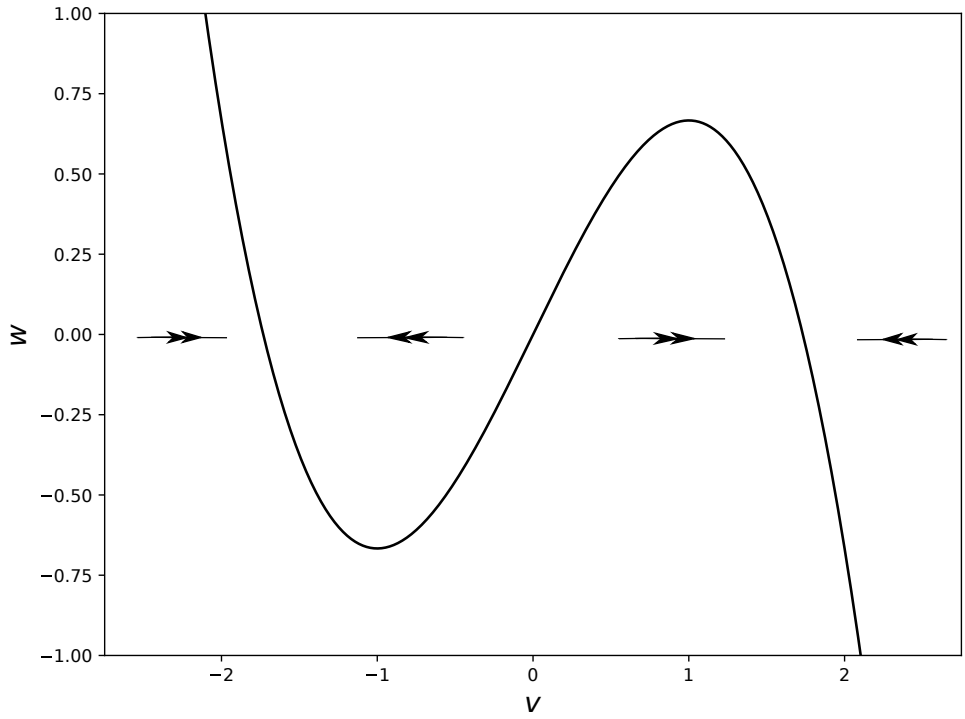

Figure 9: Critical manifold of the FitzHugh-Nagumo equations coincides with the nullcline for dv/dt. The arrow indicate the stability of the different branches of the critical manifold.